EUROPEAN ORGANIZATION FOR NUCLEAR RESEARCH

CERN-EP/99-156
November 2, 1999

Measurement of the Probability of Gluon Splitting into Charmed Quarks in Hadronic Z Decays

The L3 Collaboration

Abstract

We have measured the probability, $\overline{n}_{g\to c\bar{c}}$, of a gluon splitting into a charm-quark pair using 1.7 million hadronic Z decays collected by the L3 detector. Two independent methods have been applied to events with a three-jet topology. One method relies on tagging charmed hadrons by identifying a lepton in the lowest energy jet. The other method uses a neural network based on global event shape parameters. Combining both methods, we measure $\overline{n}_{g\to c\bar{c}} = [2.45 \pm 0.29 \pm 0.53]\%$.

Submitted to *Phys. Lett. B*

1 Introduction

The process of a gluon splitting into heavy quark pairs in hadronic Z decays, as shown in Fig. 1, provides a good test of perturbative QCD [1–4]. The energy scale of heavy quark pair production is in the perturbative QCD region, and the process is infrared safe because of the natural cutoff provided by the heavy quark mass. It should be mentioned that only the process of open heavy quark production is considered here. Measurements of hidden charm (J/ψ) production via QCD processes in Z decays have also been made [5].

The average number of heavy-quark pairs produced by gluon splitting per hadronic Z decay is defined by

$$\overline{n}_{g\to Q\overline{Q}} = \frac{N(Z \to q\bar{q}g, \quad g \to Q\overline{Q})}{N(Z \to \text{hadrons})} \quad , \tag{1}$$

where Q stands for a charm or bottom quark. The most recent theoretical predictions [4] to leading order in α_s, obtained by resumming large leading and next-to-leading logarithmic terms to all orders, give $\overline{n}_{g\to c\bar{c}} \approx 2\%$ and $\overline{n}_{g\to b\bar{b}} \approx 0.2\%$. There are previous experimental results for $\overline{n}_{g\to c\bar{c}}$ [6–9] and $\overline{n}_{g\to b\bar{b}}$ [10–12] . The uncertainty of these measurements contributes to the systematic error of electroweak measurements related to heavy quarks and is the biggest single source of systematic error in the measurement of $R_b = \Gamma_{b\bar{b}}/\Gamma_{had}$ [13]. Therefore, a good knowledge of $\overline{n}_{g\to c\bar{c}}$ and $\overline{n}_{g\to b\bar{b}}$ is important for precision tests of the Standard Model in the heavy-quark sector. In this letter, we present a measurement of $\overline{n}_{g\to c\bar{c}}$ using a high statistics sample of hadronic Z decay events collected by L3 [14] during the years 1994 and 1995. To identify events with a gluon jet, we first select three-jet events by applying a jet-finding algorithm that optimises the yield of $g \to c\bar{c}$ events. Subsequently, two methods are used to identify charm quarks from gluon splitting. The first method, the lepton analysis, searches for a lepton from semi-leptonic charm decays in the lowest energy jet. According to the JETSET Parton Shower [15] event generator, the latter has about an 80% probability of being a gluon jet for the identified three jet sample. The second method, the hadronic event shape analysis, uses a neural network technique, with input nodes consisting of several global event shape variables, to distinguish $g \to Q\overline{Q}$ events from backgrounds.

2 Three-Jet Event Selection

Hadronic events are selected by criteria similiar to the ones used for the measurement of the total hadronic cross section [16]. The number of selected hadronic events is 1.74 million, with an estimated background of 0.15% from other processes. To identify the gluon jet, we require a three-jet event topology and assume that the lowest energy jet is a gluon jet. The jets are found by the JADE algorithm [17] with a y_{cut} value of 0.03, which maximises the fraction of $g \to c\bar{c}$ events. This cut assigns 63% of $g \to c\bar{c}$ events to the three-jet topology. The jet energies are calculated using the relation:

$$E_i = E_{cm}\left[\frac{\sin\psi_{jk}}{\sin\psi_{jk} + \sin\psi_{ki} + \sin\psi_{ij}}\right] \quad , \tag{2}$$

where E_{cm} is the center of mass energy and ψ_{ij} is the angle in space between jets i and j. Planar (three jet) events are defined by the condition that the sum of the angles between the

three jets is greater than 358°. The jets are labelled in decreasing order of jet energy. To ensure that most charged particles are contained in the acceptance of the Silicon Microvertex Detector which is used to improve the event signature, the polar angle of the thrust axis, θ_{T}, must satisfy the condition: $|\cos\theta_{\mathrm{T}}| < 0.7$. With these additional criteria, 430k hadronic events are selected.

3 Lepton Analysis

3.1 $\mathrm{g} \to \mathrm{c\bar{c}}$ Event Selection and Background Sources

This method uses events with an electron or a muon candidate in the lowest energy jet to tag a charm quark from gluon splitting. Electron candidates are selected by the criteria:

- An energy cluster with electromagnetic energy greater than 2 GeV, hadronic energy less than 2 GeV and polar angle, θ, such that $|\cos\theta| < 0.72$.
- The electromagnetic energy cluster must have between 10 and 40 associated BGO crystals and more than 95% of the energy in the 9 central crystals.
- Matching is required in the azimuthal angle ϕ and transverse energy between the energy cluster and a track in the central track chamber.

For the muon candidates it is required that:

- A track is found in the barrel muon system with hits in 2 or more ϕ chamber layers and 1 or more Z-chamber layers.
- The distance of closest approach to the fill vertex in the transverse plane is less than 100 mm, as well as less than three times the estimated error due to multiple scattering in the calorimeters.

More details of the electron and muon selection criteria are given in reference [18]. The electron energy is required to be between 2 GeV and 6 GeV, while the measured muon momentum must be between 3 GeV and 6 GeV; the lepton selection gives 1000 electron and 1287 muon candidates. For background and acceptance studies, a Monte Carlo sample of 5.2 million hadronic Z decays is used. The events are generated using the JETSET 7.3 generator [15], passed through the full L3 detector simulation [19] and analysed in the same way as the data. The following backgrounds, to the $\mathrm{g} \to \mathrm{c\bar{c}}$ signal contribute, in decreasing order of importance, to the selected lepton samples:

- $\mathrm{Z} \to \mathrm{b\bar{b}}$ and $\mathrm{Z} \to \mathrm{c\bar{c}}$ events with hard gluon radiation. In this case, the lowest energy jet contains a lepton coming from a semi-leptonic decay of a primary heavy quark.
- Hadrons misidentified as lepton candidates.
- Decay in flight of $\pi^{\pm}$ or $\mathrm{K}^{\pm}$ into a muon.
- Dalitz decays: $\pi^0, \eta \to \mathrm{e^+e^-}\gamma$.
- Photon conversions into electron pairs.

- $Z \to q\bar{q}g,\ g \to b\bar{b}$.

Monte Carlo studies show that 62% of the selected events with an electron and 47% of the events with a muon contain a directly produced heavy quark, usually a b or $\bar{b}$, in the lowest energy jet. To reduce this background, we use an event discriminant variable [20], D, the negative logarithm of the probability that all tracks originate from the primary vertex, which has small values when all tracks originate from the primary vertex and large values for events containing secondary vertices. Applying the cut $D < 1.5$ rejects 58% of the b-quark background while keeping 85% of the $g \to c\bar{c}$ events. Further discrimination between gluon splitting events and directly produced b or $\bar{b}$ quarks is provided by the invariant mass of the lowest energy jet, M_{j3}; events are rejected if $M_{j3} < 6.5$ GeV.

Since all backgrounds are estimated from Monte Carlo events, we have compared several of the crucial Monte Carlo distributions with the data. For example, the muon and electron momentum, the event discriminant D, and the effective mass of the lowest energy jet, are shown in Fig. 2a-d. Good agreement is seen for all these distributions.

In order to estimate the background from jet misassignment and to check the heavy flavour composition in the data and Monte Carlo, we extract the fraction of $Z \to b\bar{b}$ events (R_b^{3jet}) in the three-jet events from data samples using a double-hemisphere tagging method [20]. The result found is $R_b^{3jet} = 0.2017 \pm 0.0027 \pm 0.0030$, where the first error is statistical and the second is systematic, mainly due to uncertainties on the hemisphere correlations and on the selection efficiencies of the light and charm quarks. This is significantly different from the untuned Monte Carlo value of 0.2146 ± 0.0003. The $Z \to b\bar{b}$ event fraction in the Monte Carlo is therefore corrected by reweighting the events according to the measured R_b^{3jet} value. The uncertaintity in the value of R_b^{3jet} is taken into account in the systematic error.

Applying the event discriminant and the third-jet invariant mass cut, the ratio between data and Monte Carlo predictions for the fraction of selected leptons in the two highest energy jets is found to be consistent with unity:

$$\frac{f_\mu^{DATA}}{f_\mu^{MC}} = 0.977 \pm 0.026, \quad \frac{f_e^{DATA}}{f_e^{MC}} = 1.025 \pm 0.053.$$

In this background enriched sample good agreement is found between data and Monte Carlo. After all selection criteria, 360 electron and 450 muon candidate events are selected in the lowest energy jet. The remaining backgrounds are estimated from Monte Carlo as shown in Table 1.

3.2 Results

After subtracting all background contributions except that due to $g \to b\bar{b}$, 51 ± 24 and 75 ± 21 $g \to Q\overline{Q}$ splitting events are found for the muon and electron channels, respectively, where the errors are statistical only. The average number of charm quark pairs from gluon splitting per hadronic event is then given by:

$$\overline{n}_{g\to c\bar{c}} = \frac{N_{sel}}{N_{had} \cdot \varepsilon^c \cdot 2 \cdot Br(c \to X\ell\nu)} - \frac{\varepsilon^b Br(b \to X\ell\nu)}{\varepsilon^c Br(c \to X\ell\nu)} \overline{n}_{g\to b\bar{b}}, \tag{3}$$

Where ε^c, ε^b are the selection efficiencies for $g \to c\bar{c}$ and $g \to b\bar{b}$ events, respectively, given in Table 2, N_{sel} is the number of events after background subtraction, N_{had} is the total number

of hadronic Z decays and $Br(\mathrm{c} \to \mathrm{X}\ell\nu)$ and $Br(\mathrm{b} \to \mathrm{X}\ell\nu)$ are the c and b hadron semileptonic branching ratios [21], given in Table 3. Using the efficiencies shown in Table 2, we obtain:

$$\begin{aligned} \overline{n}_{\mathrm{g}\to\mathrm{c\bar{c}}} &= [3.06 \pm 1.76 - 2.59(\overline{n}_{\mathrm{g}\to\mathrm{b\bar{b}}} - 0.26)]\% \quad \text{(muons)} \\ \overline{n}_{\mathrm{g}\to\mathrm{c\bar{c}}} &= [3.14 \pm 1.14 - 3.59(\overline{n}_{\mathrm{g}\to\mathrm{b\bar{b}}} - 0.26)]\% \quad \text{(electrons)} \end{aligned}$$

where the errors are from data statistics only. These results correspond to the weighted average of the published values of $\overline{n}_{\mathrm{g}\to\mathrm{b\bar{b}}}$ [10, 11] of $[0.26 \pm 0.06]\%$.

3.3 Systematic Errors

The different systematic errors for the lepton analysis are presented in Table 3. There are three distinct sources: experimental systematic errors, errors from leptonic branching ratio uncertainties and modelling errors that can affect both signal and background. The errors labelled 'Monte Carlo Statistics' originate from the limited statistics of the Monte Carlo samples of the processes $\mathrm{g} \to \mathrm{c\bar{c}}$ and $\mathrm{g} \to \mathrm{b\bar{b}}$ used to calculate the selection efficiencies ε^c and ε^b. For each cut or parameter variation all the efficiencies (including ε^b) were recalculated and used in Eqn.(3) to obtain the values of $\delta(\overline{n}_{\mathrm{g}\to\mathrm{c\bar{c}}})/\overline{n}_{\mathrm{g}\to\mathrm{c\bar{c}}}$ presented in Table 3.

The errors on the lepton detection efficiency are estimated by varying the lepton selection cuts by $\pm 10\%$ around their nominal values. The errors on the background simulation are estimated using 'lepton enriched' samples of electrons and muons. The systematic errors are estimated as the difference between data and Monte Carlo after applying the invariant mass and event discriminant cuts to these samples. This difference in the background due to misidentified hadrons, photon conversions, Dalitz decays and decays in flight amounts to 2.0% for muons and 8.1% for electrons. The 'Track Smearing' error is estimated by smearing tracks to improve the data/Monte Carlo comparison for the event discriminant. The error is the difference in the gluon splitting rate calculated with, or without, the smeared Monte Carlo. The modelling errors are estimated by varying the parameters of the JETSET parton shower model that was previously tuned to our data [22]. We vary, within their measured errors, the parameters ϵ_b and ϵ_c in the Peterson fragmentation function [23], the parameter b in the Lund symmetric fragmentation function [24] for light quarks, the parameter σ_q, describing hadron transverse momenta and the QCD scale parameter Λ_{LLA} used for the parton shower evolution. Since fully simulated events are not available with different values of these parameters, their effects are determined from generated events with a detector resolution smeared so as to be consistent with the data. The systematic error due to different models of semileptonic decays of charm and bottom is also considered. In addition to the JETSET decay model, we estimate the uncertainty by also considering the models of Altarelli *et al.*(ACCMM) [25], Isgur *et al.*(ISGW) and the modified Isgur model (ISGW**) [26]. The ACCMM model is used for the central values of our measurement.

Combining the muon and electron channels, taking into account the correlated errors arising from the leptonic branching ratios and modelling, the overall systematic error is estimated to be 21.5%, giving the result:

$$\overline{n}_{\mathrm{g}\to\mathrm{c\bar{c}}} = [3.12 \pm 0.96 \pm 0.67 - 3.28(\overline{n}_{\mathrm{g}\to\mathrm{b\bar{b}}} - 0.26)]\% \quad \text{(leptons)}$$

where the first error is statistical and the second systematic.

4 Event Shape Analysis

This analysis uses characteristic differences in event shape distributions for the gluon splitting to heavy quark process, as compared to the background processes where heavy quarks are directly produced by electroweak Z decays. The rather low purity attainable as compared to the lepton analysis is largely compensated by data statistics as all hadronic decays of heavy quarks are utilised.

4.1 $g \to Q\overline{Q}$ Event Selection

In events with a three-jet topology, most of the gluon jets radiated by a primary quark are in the two lowest energy jets. Due to the large mass of the heavy quark, a gluon jet containing a heavy quark has a larger invariant mass and energy than one containing light quarks. Hence, the distribution of the sum of the invariant masses of the two lowest energy jets and the energy fraction in a cone around the jet axis are different in a gluon jet with heavy quarks than in one with light quarks. Observables, sensitive to the correlation among the three jet momenta, can also allow a discrimination between events with a gluon splitting to heavy quark pairs and to light quarks or to gluons. In this method, we use three different categories of Monte Carlo event samples as follows:

- 80,000 events containing gluon splitting to charm quark pairs, called the C sample.
- 8,000 events with gluon splitting to bottom quark pairs, called the B sample.
- 5.2 million events without the gluon splitting to heavy quark pair process, called the N sample.

A neural network [27] has been constructed based on the following five variables:

- The difference between the sum of the invariant masses of the two lowest energy jets and the invariant mass of the highest energy jet, $\Delta m \equiv m_3 + m_2 - m_1$, where m_i is the effective mass of jet i.
- The energy in a cone of 8 degree half-angle around the jet axis of the second jet, divided by the energy of the jet.
- Three different Fox-Wolfram moments (Π_1,Π_2 and Π_3), calculated from the jet momenta, sensitive to the global event topology, as described in [28].

The neural network has five input nodes, one hidden layer of 10 nodes, and one output node. For training, we assume that the samples C and B are the signal events and the N sample is background. Subsamples of 10,000 N events, 9,000 C events and 1,000 B events are used for training. Since events with a gluon splitting into light quark pairs or gluon pairs are a major background source, we use the event discriminant variable, D, to reduce this background. Introducing a lower cut on the event discriminant variable in this analysis, the light quark background is reduced and the data sample is almost uncorrelated with the one used in the lepton analysis. Fig.3 shows the distribution of the neural network output, O, for $g \to Q\overline{Q}$ and for background after applying the cut $D > 1.0$. Optimising the total error on the signal, we choose the cut: $O > 0.59$. The corresponding selection efficiencies of the data and of the three

Monte Carlo samples are listed in Table 4. Requiring only the three-jet event selection, the purity for the $g \to c\bar{c}$ events is found to be 2.5%. After the cuts $O > 0.59$ and $D > 1.0$, the purity is increased to 4.5% and systematic uncertainties are reduced. The purity estimations given correspond to the value of 0.15% for $\overline{n}_{g\to b\bar{b}}$ used in the JETSET generator. In the region, $O > 0.59$ and $1.0 < D < 1.5$, only 35 events from the lepton analysis are found among the 9,520 selected events. The lepton and event shape analyses can therefore be considered as uncorrelated.

4.2 Results and Systematic Errors

We extract the probability of a gluon splitting into charm quark pairs using the relation:

$$\overline{n}_{g\to c\bar{c}} = \frac{\varepsilon_D - \varepsilon_N - (\varepsilon_B - \varepsilon_N)\overline{n}_{g\to b\bar{b}}}{\varepsilon_C - \varepsilon_N} \quad , \tag{4}$$

where ε_D, ε_C, ε_B and ε_N are the efficiencies for the data, C, B and N samples, respectively. The values obtained are listed in Table 4 and they yield the result:

$$\overline{n}_{g\to c\bar{c}} \;=\; [2.27 \pm 0.30 - 3.86(\overline{n}_{g\to b\bar{b}} - 0.26)]\%,$$

where the error is from data statistics only, and the dependence on $\overline{n}_{g\to b\bar{b}}$ is shown explicitly. This value is in good agreement with that obtained by the lepton analysis.

The statistical significance of the observed signal is illustrated in Fig 4. The distributions of the neural network output for the data and the background Monte Carlo are shown in Fig 4a. The relative normalisations are determined according to Eqn.(4) in the region $O > 0.59$. The corresponding $g \to Q\overline{Q}$ signal after background subtraction is shown in Fig 4b as compared to the Monte Carlo prediction normalised to the measured value of $\overline{n}_{g\to c\bar{c}}$. Although the analysis has a low purity, the gluon splitting signal is seen to be large. For the region $O > 0.59$, it amounts to 2064 $\pm$ 182 events. The hatched area in Fig 4b shows the estimated $g \to b\bar{b}$ contribution.

Systematic errors in the efficiencies arise due to imperfect modelling of the event shape distributions in the Monte Carlo. We estimate the systematic errors due to several input parameters in the JETSET Parton Shower generator by varying their values within the estimated errors. For this purpose, fast simulations which take into account the detector resolution have been performed for N, C and B samples. Comparing the efficiencies of the new samples, generated by variation of one of the parameters, to those obtained with the tuned parameter from the reference sample, the changes $\delta(\overline{n}_{g\to c\bar{c}})/\overline{n}_{g\to c\bar{c}}$, due to the uncertainties of different parameters, are found and listed in Table 5.

In addition to the tuned fragmentation parameters in JETSET, we consider the following sources of systematic error:

- Monte Carlo statistics.
- R_b^{3jet}: We correct the Monte Carlo samples by the measured value of R_b^{3jet} in three-jet events. The changes due to the measurement error on this quantity are assigned as a systematic error.
- Track smearing: This error is estimated in the same way as for the leptonic analysis (see section 3.3 above).

- Energy calibration: since we reconstruct three-jet events with calorimetric clusters, the systematic uncertainty from the energy calibration of the calorimeters is studied. We use the Monte Carlo samples of reconstructed three-jet events with energy smearing of clusters according to the nominal calorimeter resolution. We repeat the analysis and assign the difference as the error.

Our measurement is also checked by using different values of y_{cut}. With the values of 0.02 and 0.04 of y_{cut}, we measure the $\overline{n}_{g\to c\bar{c}}$ to be $(2.48 \pm 0.39)\%$ and $(2.03 \pm 0.27)\%$, respectively, where the error is only statistical. These values are very consistent with that given by the standard value $y_{cut} = 0.03$. The stability of the result to variation of the event discriminant and neural network cuts was also investigated. No systematic deviations were observed. Adding all the systematic errors in quadrature, we obtain a total systematic error of 23.7%, yielding the result:

$$\overline{n}_{g\to c\bar{c}} \;=\; [2.27 \pm 0.30 \pm 0.54 - 3.86(\overline{n}_{g\to b\bar{b}} - 0.26)]\% \;\; \text{(eventshape)}.$$

5 Combined Result and Discussion

The measurements from the two different methods are now combined in an uncorrelated manner giving the result:

$$\overline{n}_{g\to c\bar{c}} \;=\; [2.45 \pm 0.29 \pm 0.53]\% \;\; ,$$

where it is assumed that $\overline{n}_{g\to b\bar{b}} = [0.26 \pm 0.06]\%$. In the errors quoted, statistical and systematic errors (assumed uncorrelated in the two different analysis methods) are combined in quadrature. Our result is compared with other measurements and theoretical predictions in Table 6. Good agreement is found between the different experimental measurements. The latest resummed perturbative QCD calculation [4] agrees, within errors, with our measurement. Our result is also in good agreement with the prediction of the ARIADNE and JETSET generators.

Acknowledgements

We express our gratitude to the CERN accelerator divisions for the excellent performance of the LEP machine. We acknowledge with appreciation the effort of all engineers, technicians and support staff who have participated in the construction and maintenance of this experiment.

References

[1] M.L. Mangano and P. Nason, Phys. Lett. **B285** (1992) 160.

[2] M.H. Seymour, Z Phys. **C63** (1994) 99.

[3] M.H. Seymour, Nucl. Phys. **B436** (1995) 163.

[4] D.J. Miller and M.H. Seymour, Phys. Lett. **B435** (1998) 213.

[5] L3 Collab., M. Acciarri *et al.*, Phys. Lett. **B453** (1999) 94.

[6] OPAL Collab., R.Akers *et al.*, Z. Phys. **C67** (1995) 27.

[7] OPAL Collab. R. Akers *et al.*, Phys. Lett. **B353** (1995) 545.

[8] OPAL Collab., G. Abbiendi *et al.*, CERN EP/99-089, Submitted to European Physics Journal C.

[9] ALEPH Collab., R. Barate *et al.*, CERN EP/99-094, Submitted to European Physics Journal C.

[10] DELPHI Collab., P. Abreu *et al.*Phys. Lett. **B405** (1997) 202.

[11] ALEPH Collab., R. Barate *et al.*, Phys. Lett. **B434** (1998) 437.

[12] DELPHI Collab., P. Abreu *et al.*, Phys. Lett., **B462** (1999) 425.

[13] The LEP Collaborations, "A Combination of Preliminary Electroweak Measurements and Constraints on the Standard Model", CERN-EP/99-15; 08 February 1999.

[14] L3 Collab., B. Adeva *et al.*, Nucl. Inst. Meth. **A 289** (1990) 35;
M. Acciarri *et al.*, Nucl. Inst. Meth. **A 351** (1994) 300;
M. Chemarin *et al.*, Nucl. Inst. Meth. **A 349** (1994) 345;
I.C. Brock *et al.*, Nucl. Inst. Meth. **A 381** (1996) 236;
A. Adam *et al.*, Nucl. Inst. Meth. **A 383** (1996) 342.

[15] T. Sjöstrand, Comp. Phys. Comm. **39** (1986) 347;
T. Sjöstrand and M. Bengtsson, Comp. Phys. Comm. **39** (1986) 347;
T. Sjöstrand, JETSET 7.3 manual, CERN-TH6488/92 (1992).

[16] L3 Collab., B. Adeva *et al.*, Z. Phys. **C51** (1991) 179.

[17] JADE Collab., S. Bethke *et al.*, Phys. Lett. **B213** (1988) 235.

[18] L3 Collab., M. Acciarri *et al.*, Z. Phys. **C71** (1996) 379.

[19] The L3 detector simulation is based on GEANT Version 3.15.
See R. Brun *et al.*, "GEANT 3", CERN DD/EE/84-1 (Revised), September 1987.
The GHEISHA program (H. Fesefeldt, RWTH Aachen Report PITHA 85/02 (1985)) is used to simulate hadronic interactions.

[20] L3 Collab., M. Acciarri *et al.*, CERN-EP/99-121, Submitted to European Physics Journal.

[21] The LEP Electroweak Working Group, Presentation of LEP Electroweak Heavy Flavour Results for Summer 1996 Conferences 26 July 1996. L3 note 1969. LEPHF/96-01, ALEPH Note 96-099, DELPHI 96-67 PHYS 627, OPAL TN 391

[22] L3 Collab., M. Acciarri *et al.*, Z. Phys. **C55** (1992) 39;
S. Banerjee and S. Banerjee, "Tuning of the QCD Model Parameters using LEP data of Hadronic Z Decays", L3 internal note 1978, Jul. 1996.

[23] C. Peterson *et al.*, Phys. Rev. **D27** (1983) 105.

[24] B. Anderson, G. Gustafson, B. Söderberg, Z. Phys. **C20** (1983) 317.

[25] G. Altarelli *et al.*, Nucl. Phys. **B208** (1982) 365.

[26] N. Isgur *et al.*, Phys. Rev. **D39** (1989) 799.

[27] L. Lönnblad, C.Peterson and T. Rögnvaldsson, Comp. Phys. Comm. **70** (1992) 167.

[28] G.C. Fox and S. Wolfram, Phys. Lett. **B82** (1979) 134.

The L3 Collaboration:

M.Acciarri,[26] P.Achard,[19] O.Adriani,[16] M.Aguilar-Benitez,[25] J.Alcaraz,[25] G.Alemanni,[22] J.Allaby,[17] A.Aloisio,[28] M.G.Alviggi,[28] G.Ambrosi,[19] H.Anderhub,[47] V.P.Andreev,[6,36] T.Angelescu,[12] F.Anselmo,[9] A.Arefiev,[27] T.Azemoon,[3] T.Aziz,[10] P.Bagnaia,[35] L.Baksay,[42] A.Balandras,[4] R.C.Ball,[3] S.Banerjee,[10] Sw.Banerjee,[10] A.Barczyk,[47,45] R.Barillère,[17] L.Barone,[35] P.Bartalini,[22] M.Basile,[9] R.Battiston,[32] A.Bay,[22] F.Becattini,[16] U.Becker,[14] F.Behner,[47] L.Bellucci,[16] J.Berdugo,[25] P.Berges,[14] B.Bertucci,[32] B.L.Betev,[47] S.Bhattacharya,[10] M.Biasini,[32] A.Biland,[47] J.J.Blaising,[4] S.C.Blyth,[33] G.J.Bobbink,[2] A.Böhm,[1] L.Boldizsar,[13] B.Borgia,[35] D.Bourilkov,[47] M.Bourquin,[19] S.Braccini,[19] J.G.Branson,[38] V.Brigljevic,[47] F.Brochu,[4] A.Buffini,[16] A.Buijs,[43] J.D.Burger,[14] W.J.Burger,[32] A.Button,[3] X.D.Cai,[14] M.Campanelli,[47] M.Capell,[14] G.Cara Romeo,[9] G.Carlino,[28] A.M.Cartacci,[16] J.Casaus,[25] G.Castellini,[16] F.Cavallari,[35] N.Cavallo,[28] C.Cecchi,[32] M.Cerrada,[25] F.Cesaroni,[23] M.Chamizo,[19] Y.H.Chang,[49] U.K.Chaturvedi,[18] M.Chemarin,[24] A.Chen,[49] G.Chen,[7] G.M.Chen,[7] H.F.Chen,[20] H.S.Chen,[7] G.Chiefari,[28] L.Cifarelli,[37] F.Cindolo,[9] C.Civinini,[16] I.Clare,[14] R.Clare,[14] G.Coignet,[4] A.P.Colijn,[2] N.Colino,[25] S.Costantini,[8] F.Cotorobai,[12] B.Cozzoni,[9] B.de la Cruz,[25] A.Csilling,[13] S.Cucciarelli,[32] T.S.Dai,[14] J.A.van Dalen,[30] R.D'Alessandro,[16] R.de Asmundis,[28] P.Déglon,[19] A.Degré,[4] K.Deiters,[45] D.della Volpe,[28] P.Denes,[34] F.DeNotaristefani,[35] A.De Salvo,[47] M.Diemoz,[35] D.van Dierendonck,[2] F.Di Lodovico,[47] C.Dionisi,[35] M.Dittmar,[47] A.Dominguez,[38] A.Doria,[28] M.T.Dova,[18,♯] D.Duchesneau,[4] D.Dufournaud,[4] P.Duinker,[2] I.Duran,[39] H.El Mamouni,[24] A.Engler,[33] F.J.Eppling,[14] F.C.Erné,[2] P.Extermann,[19] M.Fabre,[45] R.Faccini,[35] M.A.Falagan,[25] S.Falciano,[35,17] A.Favara,[17] J.Fay,[24] O.Fedin,[36] M.Felcini,[47] T.Ferguson,[33] F.Ferroni,[35] H.Fesefeldt,[1] E.Fiandrini,[32] J.H.Field,[19] F.Filthaut,[17] P.H.Fisher,[14] I.Fisk,[38] G.Forconi,[14] L.Fredj,[19] K.Freudenreich,[47] C.Furetta,[26] Yu.Galaktionov,[27,14] S.N.Ganguli,[10] P.Garcia-Abia,[5] M.Gataullin,[31] S.S.Gau,[11] S.Gentile,[35,17] N.Gheordanescu,[12] S.Giagu,[35] Z.F.Gong,[20] G.Grenier,[24] O.Grimm,[47] M.W.Gruenewald,[8] M.Guida,[37] R.van Gulik,[2] V.K.Gupta,[34] A.Gurtu,[10] L.J.Gutay,[44] D.Haas,[5] A.Hasan,[29] D.Hatzifotiadou,[9] T.Hebbeker,[8] A.Hervé,[17] P.Hidas,[13] J.Hirschfelder,[33] H.Hofer,[47] G. Holzner,[47] H.Hoorani,[33] S.R.Hou,[49] I.Iashvili,[46] B.N.Jin,[7] L.W.Jones,[3] P.de Jong,[2] I.Josa-Mutuberría,[25] R.A.Khan,[18] D.Kamrad,[46] M.Kaur,[18,◇] M.N.Kienzle-Focacci,[19] D.Kim,[35] D.H.Kim,[41] J.K.Kim,[41] S.C.Kim,[41] J.Kirkby,[17] D.Kiss,[13] W.Kittel,[30] A.Klimentov,[14,27] A.C.König,[30] A.Kopp,[46] V.Koutsenko,[14,27] M.Kräber,[47] R.W.Kraemer,[33] W.Krenz,[1] A.Kunin,[14,27] P.Ladron de Guevara,[25] I.Laktineh,[24] G.Landi,[16] K.Lassila-Perini,[47] M.Lebeau,[17] A.Lebedev,[14] P.Lebrun,[24] P.Lecomte,[47] P.Lecoq,[17] P.Le Coultre,[47] H.J.Lee,[8] J.M.Le Goff,[17] R.Leiste,[46] E.Leonardi,[35] P.Levtchenko,[36] C.Li,[20] C.H.Lin,[49] W.T.Lin,[49] F.L.Linde,[2] L.Lista,[28] Z.A.Liu,[7] W.Lohmann,[46] E.Longo,[35] Y.S.Lu,[7] K.Lübelsmeyer,[1] C.Luci,[17,35] D.Luckey,[14] L.Lugnier,[24] L.Luminari,[35] W.Lustermann,[47] W.G.Ma,[20] M.Maity,[10] L.Malgeri,[17] A.Malinin,[27,17] C.Maña,[25] D.Mangeol,[30] P.Marchesini,[47] G.Marian,[15] J.P.Martin,[24] F.Marzano,[35] G.G.G.Massaro,[2] K.Mazumdar,[10] R.R.McNeil,[6] S.Mele,[17] L.Merola,[28] M.Meschini,[16] W.J.Metzger,[30] M.von der Mey,[1] A.Mihul,[12] H.Milcent,[17] G.Mirabelli,[35] J.Mnich,[17] G.B.Mohanty,[10] P.Molnar,[8] B.Monteleoni,[16,†] T.Moulik,[10] G.S.Muanza,[24] F.Muheim,[19] A.J.M.Muijs,[2] M.Musy,[35] M.Napolitano,[28] F.Nessi-Tedaldi,[47] H.Newman,[31] T.Niessen,[1] A.Nisati,[35] H.Nowak,[46] Y.D.Oh,[41] G.Organtini,[35] A.Oulianov,[27] C.Palomares,[25] D.Pandoulas,[1] S.Paoletti,[35,17] P.Paolucci,[28] R.Paramatti,[35] H.K.Park,[33] I.H.Park,[41] G.Pascale,[35] G.Passaleva,[17] S.Patricelli,[28] T.Paul,[11] M.Pauluzzi,[32] C.Paus,[17] F.Pauss,[47] D.Peach,[17] M.Pedace,[35] S.Pensotti,[26] D.Perret-Gallix,[4] B.Petersen,[30] D.Piccolo,[28] F.Pierella,[9] M.Pieri,[16] P.A.Piroué,[34] E.Pistolesi,[26] V.Plyaskin,[27] M.Pohl,[47] V.Pojidaev,[27,16] H.Postema,[14] J.Pothier,[17] N.Produit,[19] D.O.Prokofiev,[44] D.Prokofiev,[36] J.Quartieri,[37] G.Rahal-Callot,[47,17] M.A.Rahaman,[10] P.Raics,[15] N.Raja,[10] R.Ramelli,[47] P.G.Rancoita,[26] G.Raven,[38] P.Razis,[29] D.Ren,[47] M.Rescigno,[35] S.Reucroft,[11] T.van Rhee,[43] S.Riemann,[46] K.Riles,[3] A.Robohm,[47] J.Rodin,[42] B.P.Roe,[3] L.Romero,[25] A.Rosca,[8] S.Rosier-Lees,[4] J.A.Rubio,[17] D.Ruschmeier,[8] H.Rykaczewski,[47] S.Saremi,[6] S.Sarkar,[35] J.Salicio,[17] E.Sanchez,[17] M.P.Sanders,[30] M.E.Sarakinos,[21] C.Schäfer,[1] V.Schegelsky,[36] S.Schmidt-Kaerst,[1] D.Schmitz,[1] H.Schopper,[48] D.J.Schotanus,[30] G.Schwering,[1] C.Sciacca,[28] D.Sciarrino,[19] A.Seganti,[9] L.Servoli,[32] S.Shevchenko,[31] N.Shivarov,[40] V.Shoutko,[27] E.Shumilov,[27] A.Shvorob,[31] T.Siedenburg,[1] D.Son,[41] B.Smith,[33] P.Spillantini,[16] M.Steuer,[14] D.P.Stickland,[34] A.Stone,[6] H.Stone,[34,†] B.Stoyanov,[40] A.Straessner,[1] K.Sudhakar,[10] G.Sultanov,[18] L.Z.Sun,[20] H.Suter,[47] J.D.Swain,[18] Z.Szillasi,[42,¶] T.Sztaricskai,[42,¶] X.W.Tang,[7] L.Tauscher,[5] L.Taylor,[11] C.Timmermans,[30] Samuel C.C.Ting,[14] S.M.Ting,[14] S.C.Tonwar,[10] J.Tóth,[13] C.Tully,[34] K.L.Tung,[7] Y.Uchida,[14] J.Ulbricht,[47] E.Valente,[35] G.Vesztergombi,[13] I.Vetlitsky,[27] D.Vicinanza,[37] G.Viertel,[47] S.Villa,[11] M.Vivargent,[4] S.Vlachos,[5] I.Vodopianov,[36] H.Vogel,[33] H.Vogt,[46] I.Vorobiev,[27] A.A.Vorobyov,[36] A.Vorvolakos,[29] M.Wadhwa,[5] W.Wallraff,[1] M.Wang,[14] X.L.Wang,[20] Z.M.Wang,[20] A.Weber,[1] M.Weber,[1] P.Wienemann,[1] H.Wilkens,[30] S.X.Wu,[14] S.Wynhoff,[1] L.Xia,[31] Z.Z.Xu,[20] B.Z.Yang,[20] C.G.Yang,[7] H.J.Yang,[7] M.Yang,[7] J.B.Ye,[20] S.C.Yeh,[50] An.Zalite,[36] Yu.Zalite,[36] Z.P.Zhang,[20] G.Y.Zhu,[7] R.Y.Zhu,[31] A.Zichichi,[9,17,18] F.Ziegler,[46] G.Zilizi,[42,¶] M.Zöller.[1]

1 I. Physikalisches Institut, RWTH, D-52056 Aachen, FRG[§]
III. Physikalisches Institut, RWTH, D-52056 Aachen, FRG[§]
2 National Institute for High Energy Physics, NIKHEF, and University of Amsterdam, NL-1009 DB Amsterdam, The Netherlands
3 University of Michigan, Ann Arbor, MI 48109, USA
4 Laboratoire d'Annecy-le-Vieux de Physique des Particules, LAPP,IN2P3-CNRS, BP 110, F-74941 Annecy-le-Vieux CEDEX, France
5 Institute of Physics, University of Basel, CH-4056 Basel, Switzerland
6 Louisiana State University, Baton Rouge, LA 70803, USA
7 Institute of High Energy Physics, IHEP, 100039 Beijing, China[△]
8 Humboldt University, D-10099 Berlin, FRG[§]
9 University of Bologna and INFN-Sezione di Bologna, I-40126 Bologna, Italy
10 Tata Institute of Fundamental Research, Bombay 400 005, India
11 Northeastern University, Boston, MA 02115, USA
12 Institute of Atomic Physics and University of Bucharest, R-76900 Bucharest, Romania
13 Central Research Institute for Physics of the Hungarian Academy of Sciences, H-1525 Budapest 114, Hungary[‡]
14 Massachusetts Institute of Technology, Cambridge, MA 02139, USA
15 KLTE-ATOMKI, H-4010 Debrecen, Hungary[¶]
16 INFN Sezione di Firenze and University of Florence, I-50125 Florence, Italy
17 European Laboratory for Particle Physics, CERN, CH-1211 Geneva 23, Switzerland
18 World Laboratory, FBLJA Project, CH-1211 Geneva 23, Switzerland
19 University of Geneva, CH-1211 Geneva 4, Switzerland
20 Chinese University of Science and Technology, USTC, Hefei, Anhui 230 029, China[△]
21 SEFT, Research Institute for High Energy Physics, P.O. Box 9, SF-00014 Helsinki, Finland
22 University of Lausanne, CH-1015 Lausanne, Switzerland
23 INFN-Sezione di Lecce and Universitá Degli Studi di Lecce, I-73100 Lecce, Italy
24 Institut de Physique Nucléaire de Lyon, IN2P3-CNRS,Université Claude Bernard, F-69622 Villeurbanne, France
25 Centro de Investigaciones Energéticas, Medioambientales y Tecnologícas, CIEMAT, E-28040 Madrid, Spain[♭]
26 INFN-Sezione di Milano, I-20133 Milan, Italy
27 Institute of Theoretical and Experimental Physics, ITEP, Moscow, Russia
28 INFN-Sezione di Napoli and University of Naples, I-80125 Naples, Italy
29 Department of Natural Sciences, University of Cyprus, Nicosia, Cyprus
30 University of Nijmegen and NIKHEF, NL-6525 ED Nijmegen, The Netherlands
31 California Institute of Technology, Pasadena, CA 91125, USA
32 INFN-Sezione di Perugia and Universitá Degli Studi di Perugia, I-06100 Perugia, Italy
33 Carnegie Mellon University, Pittsburgh, PA 15213, USA
34 Princeton University, Princeton, NJ 08544, USA
35 INFN-Sezione di Roma and University of Rome, "La Sapienza", I-00185 Rome, Italy
36 Nuclear Physics Institute, St. Petersburg, Russia
37 University and INFN, Salerno, I-84100 Salerno, Italy
38 University of California, San Diego, CA 92093, USA
39 Dept. de Fisica de Particulas Elementales, Univ. de Santiago, E-15706 Santiago de Compostela, Spain
40 Bulgarian Academy of Sciences, Central Lab. of Mechatronics and Instrumentation, BU-1113 Sofia, Bulgaria
41 Center for High Energy Physics, Adv. Inst. of Sciences and Technology, 305-701 Taejon, Republic of Korea
42 University of Alabama, Tuscaloosa, AL 35486, USA
43 Utrecht University and NIKHEF, NL-3584 CB Utrecht, The Netherlands
44 Purdue University, West Lafayette, IN 47907, USA
45 Paul Scherrer Institut, PSI, CH-5232 Villigen, Switzerland
46 DESY, D-15738 Zeuthen, FRG
47 Eidgenössische Technische Hochschule, ETH Zürich, CH-8093 Zürich, Switzerland
48 University of Hamburg, D-22761 Hamburg, FRG
49 National Central University, Chung-Li, Taiwan, China
50 Department of Physics, National Tsing Hua University, Taiwan, China
§ Supported by the German Bundesministerium für Bildung, Wissenschaft, Forschung und Technologie
‡ Supported by the Hungarian OTKA fund under contract numbers T019181, F023259 and T024011.
¶ Also supported by the Hungarian OTKA fund under contract numbers T22238 and T026178.
♭ Supported also by the Comisión Interministerial de Ciencia y Tecnología.
♯ Also supported by CONICET and Universidad Nacional de La Plata, CC 67, 1900 La Plata, Argentina.
♢ Also supported by Panjab University, Chandigarh-160014, India.
△ Supported by the National Natural Science Foundation of China.
† Deceased.

Category	Muon channel	Electron channel
Observed Events	450	360
Jet misidentification	153±7	147±7
Misidentified hadrons	188±8	101±6
Photon conversions	-	2±1
Dalitz decays	-	35±4
Decays in flight	58±4	-
Total Background	399±11	285±10

Table 1: Summary of the number of selected events and the backgrounds for the lepton analysis. The quoted errors are statistical only.

Category	Muon channel	Electron channel
$\varepsilon^c(\%)$	0.40 ± 0.04	0.54 ± 0.05
$\varepsilon^b(\%)$	0.97 ± 0.10	1.81 ± 0.14

Table 2: Summary of selection efficiencies for $g \to c\bar{c}$ and $g \to b\bar{b}$ events for the lepton analysis. The quoted errors are due to Monte Carlo statistics only.

Source	$\delta(\overline{n}^{\mu}_{g\to c\bar{c}})/\overline{n}^{\mu}_{g\to c\bar{c}}(\%)$	$\delta(\overline{n}^{e}_{g\to c\bar{c}})/\overline{n}^{e}_{g\to c\bar{c}}(\%)$
Monte Carlo statistics	10.1	9.5
Lepton efficiency	6.8	7.8
Background simulation	10.0	15.0
Track smearing	1.9	3.5
Total experimental errors	15.9	19.7
$\mathrm{Br}(b\to\ell)=0.105\pm0.005$	9.8	4.1
$\mathrm{Br}(b\to c\to\ell)=0.093\pm0.007$	8.9	2.1
$\mathrm{Br}(c\to\ell)=0.098\pm0.005$	13.7	9.6
$R_b = 0.2017 \pm 0.0040$	4.0	2.9
Branching ratio errors	19.5	11.0
$\Lambda_{LLA}= 0.30 \pm 0.03$	4.3	4.9
Symmetric parameter $b = 0.76\pm0.08$	2.0	2.6
$\sigma_q= 0.39\pm0.03$	2.6	2.6
$\epsilon_b = -0.0056 \pm 0.0024$	1.6	1.6
$\epsilon_c = -0.05 \pm 0.02$	1.1	1.1
Semi-leptonic Decay model	8.2	9.3
Modelling errors	10.0	11.3
Total	27.1 [15.8]	25.2 [15.8]

Table 3: Summary of systematic errors for the muon and electron analysis. The correlated error due to branching ratios and QCD modelling is given in square brackets in the last line.

Event Category	Efficiency(%)
Data	$\varepsilon_D = 1.509 \pm 0.009$
N Sample	$\varepsilon_N = 1.411 \pm 0.006$
C Sample	$\varepsilon_C = 4.401 \pm 0.082$
B Sample	$\varepsilon_B = 12.967 \pm 0.470$

Table 4: Summary of the selection efficiencies in data and Monte Carlo for the event shape analysis. The quoted errors are due to Monte Carlo statistics only.

Source	$\delta(\overline{n}_{g\to c\bar{c}})/\overline{n}_{g\to c\bar{c}}(\%)$
MC statistics	9.2
$R_b = 0.2017 \pm 0.0040$	14.4
Track smearing	2.7
Energy calibration	12.5
$\Lambda_{LLA} = 0.30 \pm 0.03$	4.8
$\sigma_q = 0.39 \pm 0.03$	7.6
Symmetric parameter $b = 0.76 \pm 0.08$	1.7
$\epsilon_b = -0.0056 \pm 0.0024$	2.9
$\epsilon_c = -0.05 \pm 0.02$	3.8
Total	23.7

Table 5: Summary of systematic errors for the event shape analysis.

Experimental measurements of $\overline{n}_{g\to c\bar{c}}$		
Expt.	Ref.	$\overline{n}_{g\to c\bar{c}}$ (%)
L3	This paper	$2.45 \pm 0.29 \pm 0.53$
OPAL	8	$3.20 \pm 0.21 \pm 0.38$
ALEPH	9	$3.23 \pm 0.48 \pm 0.53$
Theoretical predictions for $\overline{n}_{g\to c\bar{c}}$		
Model	Ref.	$\overline{n}_{g\to c\bar{c}}$ (%)
LO pQCD	1	0.607
Resummed LO pQCD (A)	3	1.35
Resummed LO pQCD (B)	4	2.01
HERWIG	3	0.923
JETSET	3	1.70
ARIADNE	3	2.18

Table 6: Summary of published experimental measurements on $\overline{n}_{g\to c\bar{c}}$ and theoretical predictions from perturbative QCD calculations (pQCD) and Monte Carlo models (HERWIG, JETSET and ARIADNE).

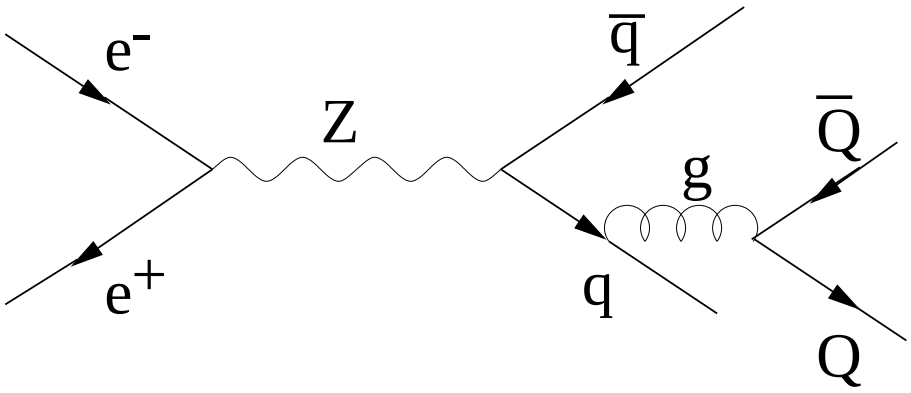

Figure 1: The lowest-order Feynman diagram for a gluon splitting into heavy-quark pairs, where Q represents a charm or bottom quark.

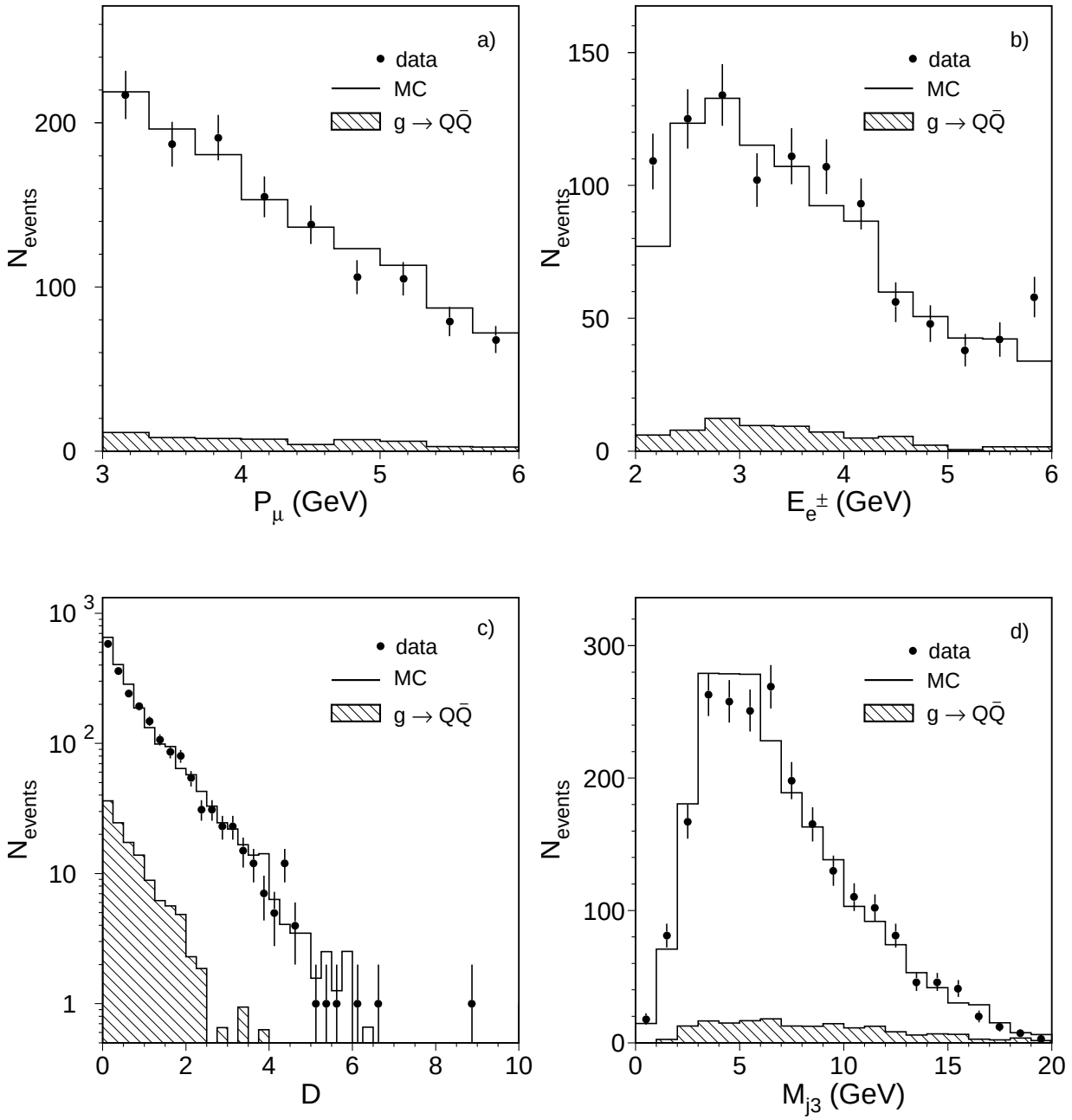

Figure 2: Distributions of: a) the momentum of the muon candidates and b) the energy of electron candidates in the lowest energy jet, c) the event discriminant, D, and d) the invariant mass of the lowest energy jet. Data are points with error bars and the open histogram is the JETSET Monte Carlo prediction. The shaded histogram shows the JETSET prediction for $g \to Q\overline{Q}$.

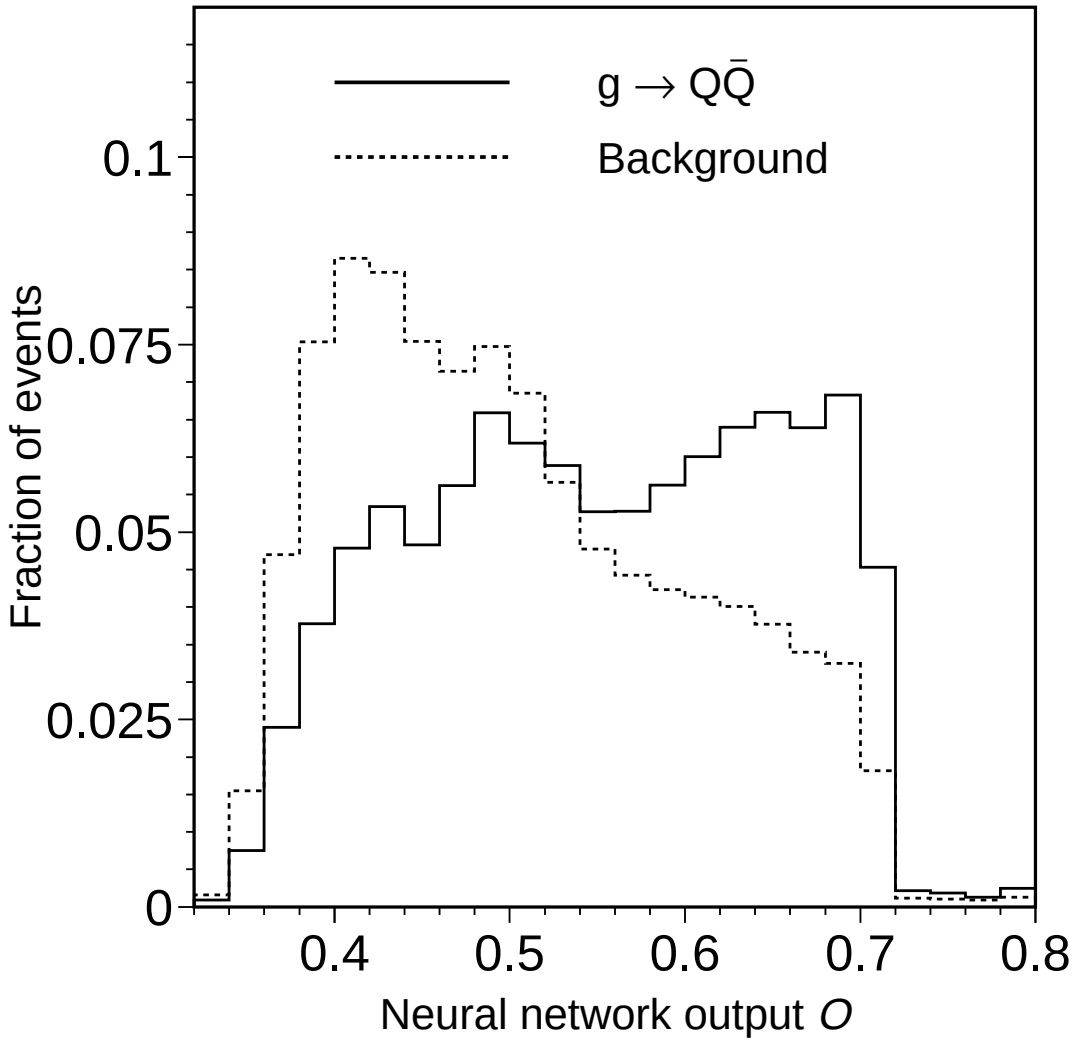

Figure 3: Neural network output distribution for g $\rightarrow$ Q$\overline{\text{Q}}$ (solid line) and background events (dashed line). The distributions are normalised to the same area.

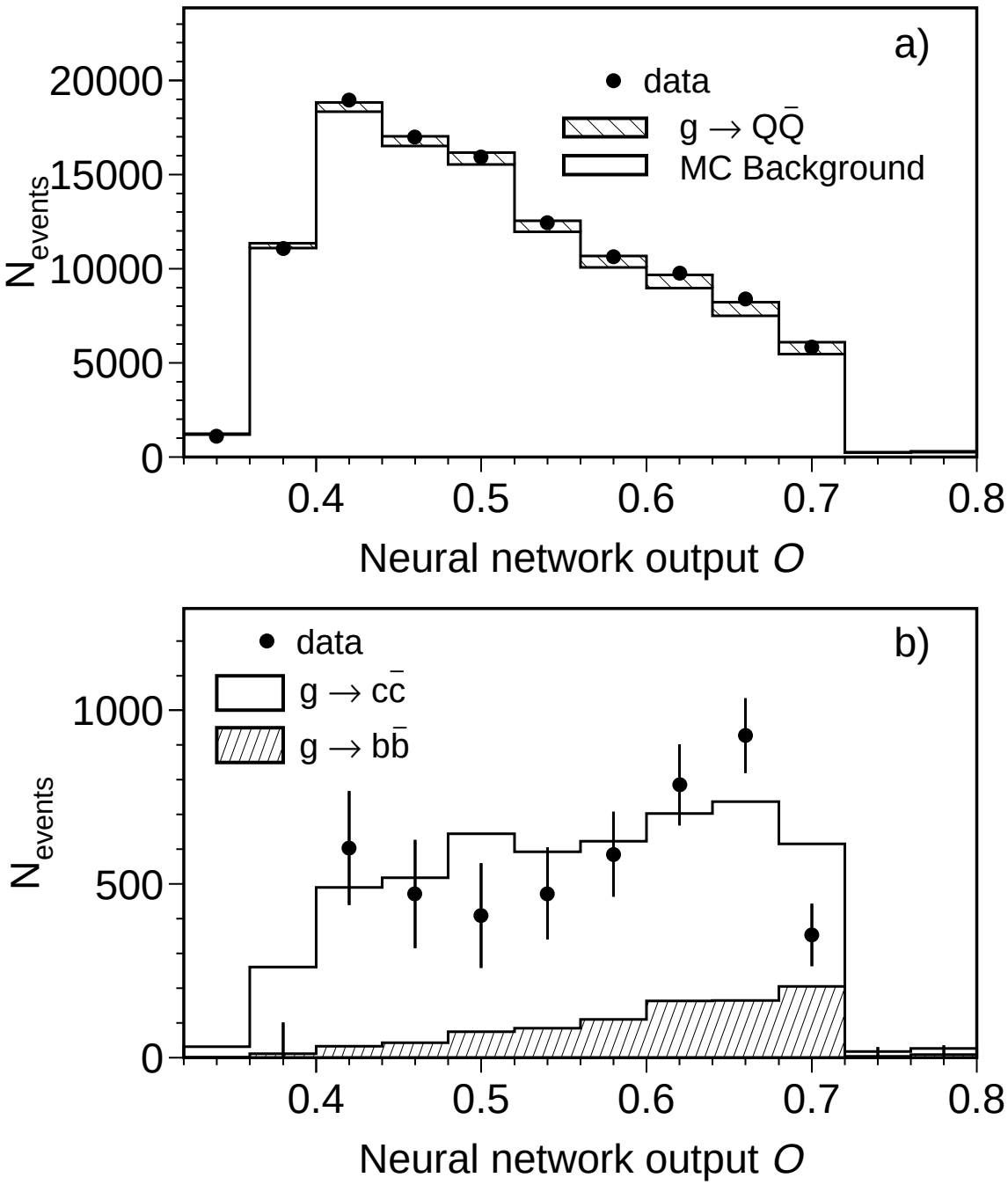

Figure 4: a) Distribution of the neural network output for data (points), background (histogram) and $g \to Q\overline{Q}$ events (hatched area). b) background-subtracted neural network output distribution for data (points) and Monte Carlo $g \to Q\overline{Q}$ events (histogram). The hatched area shows the $g \to b\bar{b}$ contribution. The contributions of $g \to c\bar{c}$ Monte Carlo events in a) and b) are normalised to the measured value of $\overline{n}_{g\to c\bar{c}}$ and the contributions of $g \to b\bar{b}$ events are estimated using the measured value of $\overline{n}_{g\to b\bar{b}}$.